

Study of the running coupling constant in 10-flavor QCD with the Schrödinger functional method

N. Yamada^{a,b}, M. Hayakawa^c, K.-I. Ishikawa^d, Y. Osaki^d, S. Takeda^e, and S. Uno^c

^a *KEK Theory Center, Institute of Particle and Nuclear Studies, High Energy Accelerator Research Organization (KEK), Tsukuba 305-0801, Japan*

^b *School of High Energy Accelerator Science, The Graduate University for Advanced Studies (Sokendai), Tsukuba 305-0801, Japan*

^c *Department of Physics, Nagoya University, Nagoya 464-8602, Japan*

^d *Department of Physics, Hiroshima University, Higashi-Hiroshima 739-8526, Japan*

^e *School of Mathematics and Physics, College of Science and Engineering, Kanazawa university, Kakuma-machi, Kanazawa, Ishikawa 920-1192, Japan*

The electroweak gauge symmetry is allowed to be spontaneously broken by the strongly interacting vector-like gauge dynamics. When the gauge coupling of a theory runs slowly in a wide range of energy scale, the theory is a candidate for walking technicolor. This may open up the possibility that the origin of all masses may be traced back to the gauge theory. We use the Schrödinger functional method to see whether the gauge coupling of 10-flavor QCD “walks” or not. Preliminary result is reported.

Keywords: Lattice Gauge Theory;LHC.

1. Introduction

The main goal of Large Hadron Collider (LHC) is to confirm the Higgs mechanism and to find particle contents and the physics law above the electroweak scale. So far many new physics models beyond the standard model have been proposed. Among them, Technicolor (TC)¹ is one of the most attractive candidates² as it does not require elementary scalar particles which cause, so-called, the fine-tuning problem. This model is basically a QCD-like, strongly interacting vector-like gauge theory. Therefore, lattice gauge theory provides the best way to study this class of model,³ and the predictions can be as precise as those for QCD, in principle.

The simple, QCD-like TC model, *i.e.* an SU(3) gauge theory with two or three flavors of techniquarks, has been already ruled out by, for instance, the S-parameter⁴ and the FCNC constraints. However, it has been argued that, if the gauge coupling runs very slowly (“walks”) in a wide range of energy scale before spontaneous chiral symmetry breaking occurs, at least, the FCNC problem may disappear.⁵ Such TC models are called walking technicolor (WTC) and several explicit candidates are discussed in semi-quantitative manner in Ref.⁶ Since the dynamics in WTC might be completely different from that in QCD and hence the use of the naive scaling

in N_c or N_f to estimate various quantities may not work, the S -parameter must be evaluated from the first principles.⁷ Although really important quantity is the anomalous dimension of $\bar{\psi}\psi$ operator, looking for theories showing the walking behavior is a good starting point. Recently many groups started quantitative studies using lattice technique to answer the question what gauge theory shows walking behavior. In Ref.,⁸ the running couplings of 8- and 12-flavor QCD are studied on the lattice using the Schrödinger functional (SF) scheme.⁹ Their conclusion is that while 8-flavor QCD does not show walking behavior 12-flavor QCD reaches an infrared fixed point (IRFP) at $g_{\text{IR}}^2 \sim 5$. In spite of the scheme-dependence of running and its value of IRFP, the speculation inferred from Schwinger-Dyson equation¹⁰ suggests that $g_{\text{IR}}^2 \sim 5$ is not large enough to trigger spontaneous chiral symmetry breaking. Although 12-flavor QCD is still an attractive candidate and is open to debate,¹¹ we explore other N_f . In the following, we report the preliminary results on the running coupling in 10-flavor QCD. Since the conference, statistics and analysis method are changed. The following analysis is based on the increased statistics and a slightly different analysis method.

2. Perturbative analysis

Before going into the simulation details, let us discuss some results from perturbative analysis. In this work, we adopt the β function defined by

$$\beta(g^2(L)) = L \frac{\partial g^2(L)}{\partial L} = b_1 g^4(L) + b_2 g^6(L) + b_3 g^8(L) + b_4 g^{10}(L) + \dots, \quad (1)$$

where L denotes a length scale. The first two coefficients are scheme-independent, and given by

$$b_1 = \frac{2}{(4\pi)^2} \left[11 - \frac{2}{3} N_f \right], \quad b_2 = \frac{2}{(4\pi)^4} \left[102 - \frac{38}{3} N_f \right]. \quad (2)$$

Other higher order coefficients are scheme-dependent and are known only in the limited schemes and orders. In this section, we analyze the perturbative running in the four different schemes/approximations: i) two-loop (universal), ii) three-loop in the $\overline{\text{MS}}$ scheme, iii) four-loop in the $\overline{\text{MS}}$ scheme, iv) three-loop in the Schrödinger functional scheme. The perturbative coefficients relevant to the following analysis are

$$b_3^{\overline{\text{MS}}} = \frac{2}{(4\pi)^6} \left[\frac{2857}{2} - \frac{5033}{18} N_f + \frac{325}{54} N_f^2 \right], \quad (3)$$

$$b_4^{\overline{\text{MS}}} = \frac{2}{(4\pi)^8} \left[29243.0 - 6946.30 N_f + 405.089 N_f^2 + 1.49931 N_f^3 \right], \quad (4)$$

$$b_3^{\text{SF}} = b_3^{\overline{\text{MS}}} + \frac{b_2 c_2^\theta}{2\pi} - \frac{b_1 (c_3^\theta - c_2^{\theta^2})}{8\pi^2}, \quad (5)$$

N_f	4	6	8	10	12	14	16
2-loop universal				27.74	9.47	3.49	0.52
3-loop SF	43.36	23.75	15.52	9.45	5.18	2.43	0.47
3-loop $\overline{\text{MS}}$		159.92	18.40	9.60	5.46	2.70	0.50
4-loop $\overline{\text{MS}}$			19.47	10.24	5.91	2.81	0.50

Tab. 1 The IRFP from perturbative analysis.

where the coefficients c_2^θ and c_3^θ depend on the spatial boundary condition of the SF used in calculations, *i.e.* θ . Those for $\theta = \pi/5$ and c_2^θ for $\theta = 0$ are known as

$$c_2^{\theta=\pi/5} = 1.25563 + 0.039863 \times N_f, \quad (6)$$

$$c_3^{\theta=\pi/5} = (c_2^{\theta=\pi/5})^2 + 1.197(10) + 0.140(6) \times N_f - 0.0330(2) \times N_f^2, \quad (7)$$

$$c_2^{\theta=0} = 1.25563 + 0.022504 \times N_f, \quad (8)$$

but $c_3^{\theta=0}$ is not. Therefore, the case iv) is studied with $\theta=\pi/5$. Notice that in our numerical simulation $\theta=0$ and thus, rigorously speaking, the example iv) is not applied to our numerical result.

The perturbative infrared fixed point (IRFP) are numerically solved and summarized in Tab. 1. As seen from Tab. 1, with $N_f \geq 8$ the fixed point value is, to some extent, stable against the change of schemes/approximations. It is interesting that the IRFP of 12-flavor QCD in the SF scheme is consistent with the non-perturbative calculation by Ref.⁸ Now looking at the perturbative IRFP at $N_f = 10$, it appears to be stable at $g^2 \sim 10$. Furthermore, according to the analysis based on Schwinger-Dyson equation, there is an argument that chiral symmetry breaking occurs at around $g^2 \sim 4\pi^2/(3C_2(R)) = \pi^2$.¹⁰ In summary, the perturbative analysis suggests that 10-flavor QCD is the most attractive candidate for WTC.

3. Simulation parameters and setup

We employ the Schrödinger functional method⁹ to calculate the running coupling constant. Unimproved Wilson fermion action and the standard plaquette gauge action without any boundary counter terms are used. The parameter of the spatial boundary condition for fermions, θ , is set to zero. The bare gauge coupling $\beta = 6/g_0^2$ is explored in the range of 4.4–24.0. In this analysis, we report the results obtained from $(L/a)^4 = 6^4, 8^4$ and 12^4 lattices. The calculation on 16^4 lattice is in progress. The numerical simulation is carried out on several architectures including GPGPU and PC cluster. The standard HMC algorithm is used with some improvements in the solver part like the mixed precision algorithm. So far, we have accumulated 5,000 to 200,000 trajectories depending on $(\beta, L/a)$.

Since the Wilson type fermion explicitly violates chiral symmetry, the critical value of κ has to be tuned to the massless limit. We performed this tuning for every pair of $(\beta, L/a)$. At around $\beta \sim 4.4$, for massless fermions we encounter a (probably first order) phase transition independently of L/a , where the plaquette

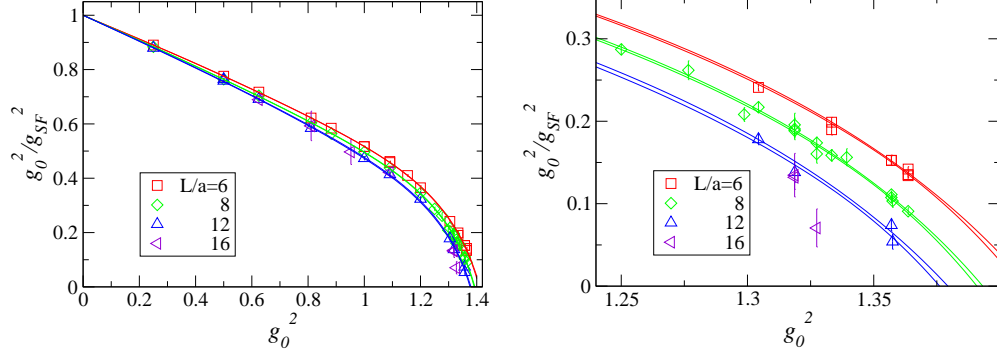


Fig. 1. g_0^2 -dependence of $g_0^2/g_{\text{SF}}^2(L)$ at $L/a = 6, 8, 12, 16$. The right panel enlarges the region of $g_0^2 \in [1.25, 1.40]$ of the left.

value suddenly jumps to a smaller value. Since this bulk phase transition is inferred to be lattice artifact, whenever this happens we discard the configurations. Thus the position of the critical β (~ 4.4) sets the lower limit on β at which simulations make sense.

4. Preliminary results

Figure 1 shows the Schrödinger functional coupling calculated on the lattices, where g_0^2/g_{SF}^2 is plotted as a function of the bare coupling. The solid curve is the result (and statistical error) of the fit to

$$\frac{g_0^2}{g_{\text{SF}}^{\text{lat}^2}(g_0^2, L/a)} = \frac{1 - a_{L/a,1} g_0^4}{1 + p_{1,L/a} \times g_0^2 + \sum_{n=2}^N a_{L/a,n} \times g_0^{2n}}, \quad (9)$$

where $p_{1,L/a}$ is the L/a -dependent coefficient and is found, by perturbative calculation, to be

$$p_{1,L/a} = \begin{cases} 0.4477107831 & \text{for } L/a = 6 \\ 0.4624813408 & \text{for } L/a = 8 \\ 0.4756888260 & \text{for } L/a = 12 \end{cases}. \quad (10)$$

We optimize the degree of polynomial N in the denominator of (9) by monitoring χ^2/dof , and take $N = 5$ for $L/a = 6$ and $N = 4$ for $L/a = 8, 12$.

Since we do not implement any $O(a)$ improvements, large scaling violation is expected to exist. One promising prescription to improve discretization errors has been proposed in Ref.¹² Let us parameterize the lattice artifact in the step scaling by

$$\delta(u, s, L/a) = \frac{\frac{\Sigma_0(u, s, L/a)}{1 + \delta^{(1)}(s, L/a)u} - \sigma(u, s)}{\sigma(u, s)} = \delta^{(2)}(s, L/a)u^2 + \dots, \quad (11)$$

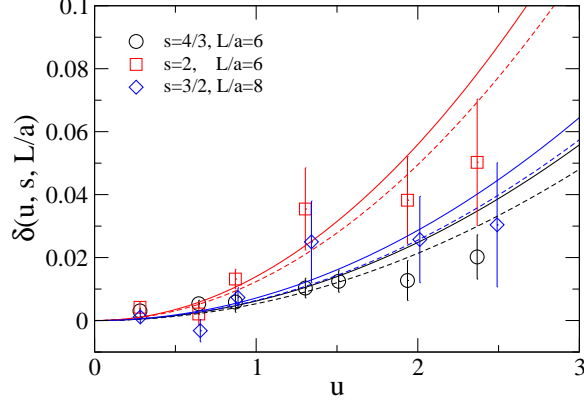


Fig. 2. δ as a function of u . $\delta^{(2)}(u, s, L/a)$ is determined as a coefficient of the quadratic term in u . (solid and dashed curves are obtained from different fit ranges.)

where $u = g_{\text{SF}}^2(L)$, $\sigma(u, s) = g_{\text{SF}}^2(sL)$ and $\Sigma_0(u, s, L/a)$ is $g_{\text{SF}}^{\text{lat}^2}(g_0^2, sL/a)$ at g_0^2 satisfying $g_{\text{SF}}^{\text{lat}^2}(g_0^2, L/a) = u$.

The coefficient $\delta^{(1)}(s, L/a)$ in eq. (11) is given by

$$\delta^{(1)}(s, L/a) = \left(p_{1, sL/a} - b_1 \ln(sL/a) \right) - \left(p_{1, L/a} - b_1 \ln(L/a) \right). \quad (12)$$

Dividing the lattice data $\Sigma_0(u, s, L/a)$ by the factor $(1 + \delta^{(1)}(s, L/a))$ improves the $O(u)$ discretization error and hence $\delta(u, s, L/a)$ starts from $O(u^2)$ as already indicated in eq. (11).

$\sigma(u, s)$ has perturbative expansion,

$$\sigma(u, s) = u + s_0 u^2 + s_1 u^3 + s_2 u^4 + s_3 u^5 + \dots, \quad (13)$$

$$s_0 = b_1 \ln(s), \quad s_1 = \ln(s) (b_1^2 \ln(s) + b_2), \quad (14)$$

$$s_2 = \ln(s) \left(b_1^3 \ln^2(s) + \frac{5}{2} b_1 b_2 \ln(s) + b_3 \right), \quad (15)$$

$$s_3 = \ln(s) \left\{ b_1^4 \ln^3(s) + \frac{13}{3} b_1^2 b_2 \ln^2(s) + \ln(s) \left(3b_1 b_3 + \frac{3}{2} b_2^2 \right) + b_4 \right\}, \quad (16)$$

where b_i 's are the coefficients of the β -function introduced in sec. 2. Since we know the first two coefficients b_1 and b_2 and hence $\sigma(u, s)$ can be numerically determined to $O(u^3)$, with such σ the $O(u^2)$ term in $\delta(u, s, L/a)$ is attributed to discretization error. The coefficient of u^2 term, $\delta^{(2)}(s, L/a)$, is then obtained by fitting $\delta(u, s, L/a)$ to a quadratic function of u . This fit must be done in the small-coupling region where the perturbative series is reliable. Since at this moment we have only a limited number of data points in such a region, the fit range is forced to extend to $u \sim 2.5$.

Figure 2 shows the u dependence of $\delta(u, s, L/a)$ and the fit results. The obtained

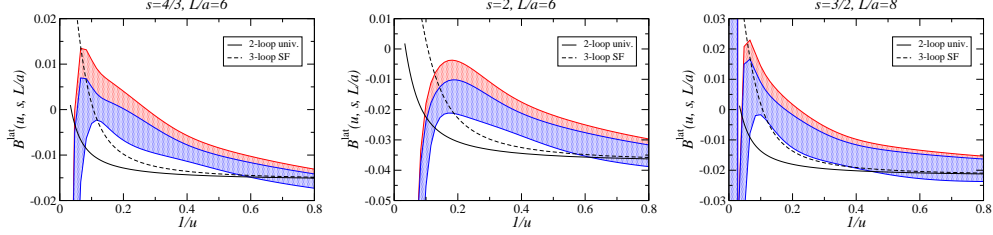


Fig. 3. Discrete beta functions for $(s, L/a)=(4/3, 6)$, $(2, 6)$ and $(3/2, 8)$ from left to right. Two colored bands are the results with statistical error, obtained by the two-loop improvement with eq. (17) (red) and eq. (18) (blue), respectively. The black solid (dashed) curve is the corresponding discrete beta function obtained by integrating perturbative two-loop universal (three-loop SF scheme) beta function.

coefficients are

$$\delta^{(2)}(s, L/a) = \begin{cases} 0.0062(9) & \text{for } s = 4/3, L/a = 6 \\ 0.0138(26) & \text{for } s = 2, L/a = 6 \\ 0.0070(24) & \text{for } s = 3/2, L/a = 8 \end{cases}, \quad (17)$$

$$\delta^{(2)}(s, L/a) = \begin{cases} 0.0053(8) & \text{for } s = 4/3, L/a = 6 \\ 0.0122(21) & \text{for } s = 2, L/a = 6 \\ 0.0062(19) & \text{for } s = 3/2, L/a = 8 \end{cases}. \quad (18)$$

In the fit, two different fit ranges, $u \in [0, 2.02]$ and $[0, 2.50]$, are applied to examine the fit range dependence of the result. Eqs. (17) and eq. (18) correspond to the former and the latter fit range, respectively. Using $\delta^{(2)}(s, L/a)$ thus extracted, we define the improved lattice data by

$$\Sigma^{\text{imp}}(u, s, L/a) = \frac{\Sigma_0(u, s, L/a)}{1 + \delta^{(1)}(s, L/a)u + \delta^{(2)}(s, L/a)u^2}. \quad (19)$$

To see the running in detail, we introduce the discrete beta function,¹³

$$B^{\text{lat}}(u, s, L/a) = \frac{1}{\Sigma^{\text{imp}}(u, s, L/a)} - \frac{1}{u}. \quad (20)$$

Figure 3 shows the $1/u$ dependence of $B^{\text{lat}}(u, s, L/a)$. As usual β function, large negative value of B^{lat} means rapid increase with length scale of the coupling, and B^{lat} flipping the sign indicate the existence of IRFP. As seen from the figure, in either pairs of $(s, L/a)$ the discrete beta function approaches to zero from below when $1/u$ decreases from 0.8 to 0.2, and this happens independently of the choice of $\delta^{(2)}$. This means that at around $u=1.25$ the running starts to slow down, *i.e.* “walk”. In order to confirm that this behavior persists even in the continuum limit, simulations on a larger lattice is necessary.

5. Summary

The running coupling constant of 10-flavor QCD is studied. The perturbative analysis suggests that this theory is extremely interesting. The preliminary result ob-

tained without continuum limit seems to indicate the walking behavior. In order to draw definite conclusions, we clearly need larger lattices to take the continuum limit. Such calculations are in progress.

A part of numerical simulations is performed on Hitachi SR11000 and the IBM System Blue Gene Solution at High Energy Accelerator Research Organization (KEK) under a support of its Large Scale Simulation Program (No. 09-05), on GCOE (Quest for Fundamental Principles in the Universe) cluster system at Nagoya University and on the INSAM (Institute for Numerical Simulations and Applied Mathematics) GPU cluster at Hiroshima University. This work is supported in part by the Grant-in-Aid for Scientific Research of the Japanese Ministry of Education, Culture, Sports, Science and Technology (Nos. 20105001, 20105002, 20105005, 21684013, 20540261 and 20740139), and by US DOE grant #DE-FG02-92ER40699.

References

1. S. Weinberg, Phys. Rev. D **13**, 974 (1976); L. Susskind, Phys. Rev. D **20**, 2619 (1979);
2. For a recent review, see, for example, C. T. Hill and E. H. Simmons, Phys. Rept. **381**, 235 (2003) [Erratum-ibid. **390**, 553 (2004)]; F. Sannino, arXiv:0804.0182 [hep-ph].
3. For recent review, see, for example, G. T. Fleming, PoS **LATTICE2008**, 021 (2008) [arXiv:0812.2035 [hep-lat]]; E. Pallante, in these proceedings.
4. M. E. Peskin and T. Takeuchi, Phys. Rev. Lett. **65**, 964 (1990); Phys. Rev. D **46**, 381 (1992).
5. B. Holdom, Phys. Rev. D **24**, 1441 (1981); K. Yamawaki, M. Bando and K. i. Matumoto, Phys. Rev. Lett. **56**, 1335 (1986); T. W. Appelquist, D. Karabali and L. C. R. Wijewardhana, Phys. Rev. Lett. **57**, 957 (1986); T. Akiba and T. Yanagida, Phys. Lett. B **169**, 432 (1986); M. Bando, T. Morozumi, H. So and K. Yamawaki, Phys. Rev. Lett. **59**, 389 (1987).
6. D. D. Dietrich and F. Sannino, Phys. Rev. D **75**, 085018 (2007) [arXiv:hep-ph/0611341].
7. E. Shintani *et al.* [JLQCD Collaboration], Phys. Rev. Lett. **101**, 242001 (2008); P. A. Boyle *et al.* [RBC and UKQCD collaborations], arXiv:0909.4931 [hep-lat].
8. T. Appelquist, G. T. Fleming and E. T. Neil, Phys. Rev. Lett. **100**, 171607 (2008); Phys. Rev. D **79**, 076010 (2009).
9. M. Luscher, R. Narayanan, P. Weisz and U. Wolff, Nucl. Phys. B **384** (1992) 168; M. Luscher, R. Sommer, P. Weisz and U. Wolff, Nucl. Phys. B **413**, 481 (1994); S. Sint and R. Sommer, Nucl. Phys. B **465**, 71 (1996); M. Luscher and P. Weisz, Nucl. Phys. B **479**, 429 (1996); A. Bode, P. Weisz and U. Wolff [ALPHA collaboration], Nucl. Phys. B **576**, 517 (2000) [Erratum-ibid. B **600**, 453 (2001 ERRAT,B608,481.2001)].
10. T. Appelquist, K. D. Lane and U. Mahanta, Phys. Rev. Lett. **61**, 1553 (1988); A. G. Cohen and H. Georgi, Nucl. Phys. B **314**, 7 (1989).
11. For the works suggesting the other possibility, see, for example, A. Hasenfratz, Phys. Rev. D **80**, 034505 (2009) [arXiv:0907.0919 [hep-lat]]; X. Y. Jin and R. D. Mawhinney, arXiv:0910.3216 [hep-lat].
12. S. Aoki *et al.* [PACS-CS Collaboration], JHEP **0910**, 053 (2009) [arXiv:0906.3906 [hep-lat]].
13. Y. Shamir, B. Svetitsky and T. DeGrand, Phys. Rev. D **78**, 031502 (2008) [arXiv:0803.1707 [hep-lat]].